



HAL
open science

Environmental Impact of Modular Power Electronics Systems Considering Diagnostic-Driven Unit Replacement

Briac Baudais, H. Ben Ahmed, Gurvan Jodin, Nicolas Degrenne, Stéphane Lefebvre

► **To cite this version:**

Briac Baudais, H. Ben Ahmed, Gurvan Jodin, Nicolas Degrenne, Stéphane Lefebvre. Environmental Impact of Modular Power Electronics Systems Considering Diagnostic-Driven Unit Replacement. PCIM Europe 2024, Jun 2024, Nuremberg, Germany. hal-04607579

HAL Id: hal-04607579

<https://hal.science/hal-04607579v1>

Submitted on 10 Jun 2024

HAL is a multi-disciplinary open access archive for the deposit and dissemination of scientific research documents, whether they are published or not. The documents may come from teaching and research institutions in France or abroad, or from public or private research centers.

L'archive ouverte pluridisciplinaire **HAL**, est destinée au dépôt et à la diffusion de documents scientifiques de niveau recherche, publiés ou non, émanant des établissements d'enseignement et de recherche français ou étrangers, des laboratoires publics ou privés.

Environmental Impact of Modular Power Electronics Systems Considering Diagnostic-Driven Unit Replacement.

Briac Baudais^{1,2}, Hamid Ben Ahmed¹, Gurvan Jodin¹, Nicolas Degrenne², Stéphane Lefebvre³

¹ SATIE, UMR CNRS 8029, École normale supérieure de Rennes, 35170 Bruz, France

² Mitsubishi Electric R&D Centre Europe, 35700 Rennes, France

³ SATIE, UMR CNRS 8029, CNRS, CNAM, Paris, France

Corresponding author: Briac Baudais, briac.baudais@ens-rennes.fr

Speaker: Briac Baudais, briac.baudais@ens-rennes.fr

Abstract

The combination of modularity and diagnosability is a natural candidate for mitigating environmental impacts (EI) throughout the lifecycle. This article proposes a method for quantifying Life Cycle Assessment (LCA), tailored to a power electronics product composed of power devices and gate drivers. It considers the effects of both modularity and diagnosability on the repair with replacement units (RU).

The results highlight that modularity and diagnosability are not relevant when several RU are subjected to failure almost concurrently (typically wearout failures of similar components), and need to be replaced during the intended lifespan. However, their significance is notable for faults qualified as "random" or "early", as these faults do not necessarily manifest throughout several RU. In certain situation involving this type of faults, system modularity and diagnostic accuracy can prove beneficial when implemented together, leading to a reduction in total EI over the service life, especially when considering mineral and metal resource depletion.

1 Introduction

The goal of considering modularity and diagnostic techniques is to allow a more precise system reparation in case of failure. Indeed, modularity allows for the replacement of only the faulty parts, and diagnostics identify which modules to replace. Since the parts that remain operational after a failure are retained, there is no need to remanufacture the entire system, thus limiting the impacts due to manufacturing.

Modularity, considered a pillar of the circular economy [1], is increasingly favored to enhance the sustainability, reparability, and recyclability of products. The question then is to quantify the environmental gain from the addition of modularity and diagnosability. The evolution of EI over time for a PE system can be represented as in Figure 1. Initially, there are EI from the product's manufacturing. Then, the slope represents the EI during usage, i.e., losses during operation. Furthermore, in the event of a fault, EI increases, corresponding to the replacement of the faulty part. Diagnostics and architecture

(modularity) influence this jump. The more precise the diagnostics, the more the replacement is limited to the component affected by the fault, provided there is modularity allowing for it. An integrated architecture does not allow for separating the faulty component from the rest.

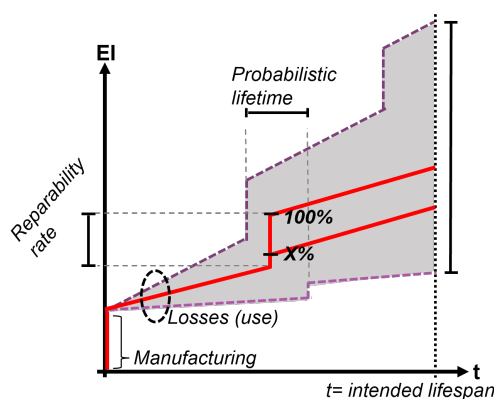


Fig. 1: Staircase curve.

This paper first presents the consideration of modularity and diagnosability in PE, then a generic method for quantifying EI. Finally, it proposes a case study, using the method, to highlight the rel-

evance of these two characteristics in determining EI over the lifecycle.

2 Modularity and diagnostic in power electronics

2.1 Modularity

The development of PE systems has been marked by complex evolutions aimed at optimizing various parameters such as cost, efficiency, and robustness. This optimization leads to different product structures. Currently, in EV applications, integrated power modules, comprising all the power semiconductor switches of the inverter predominate [2], offering high efficiency and optimal power conversion. However, this integration can result in a total system loss if a part fails, due to the inability to separate the faulty part from the rest, which can impact EI over the lifecycle.

Modularity involves reducing integration (bringing together, in the same volume and on the same substrate, all the constituent elements of the converter [3]). High integration makes repair more difficult in case of failure. The power module solution is highly integrated, as all 6 chips are located on the same substrate, the DCB. There are more modular solutions achieved by playing on integration, such as using discrete components, which only contain a single chip. Figure 2 shows different types of integration at the conversion cell level for electric vehicle inverters.

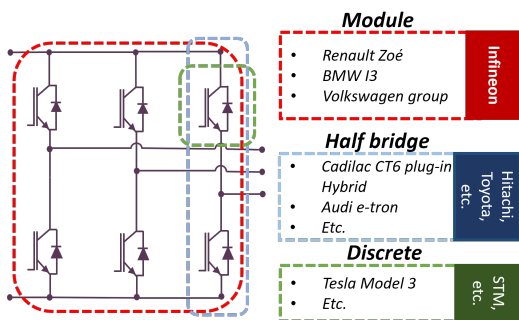


Fig. 2: Different design choices for inverter integration of electric vehicles [2].

Other modular structures exist, achieved by playing on design [4], which either allow the separation of functionalities into blocks or a matrix view of the converter.

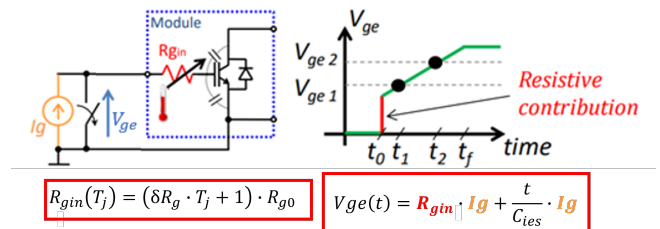
2.2 Diagnostic

Diagnosability is of crucial importance, coupled with modularity to ensure specific fault repairs. Before

exploring the various diagnostic techniques available, let us examine a common protection measure implemented in converters, as it can guide the diagnostic process.

Desaturation protection (desat) is frequently integrated to detect short circuits [5], a critical fault for power components. This mechanism reacts quickly by cutting off the control of a component when a desaturation threshold voltage is reached. This protection provides useful information for diagnosis in case of triggering during a fault.

Regarding diagnosis, attention must be paid to techniques for monitoring the lifespan of active components in PE. Various methodologies have emerged over the years [6]. Among them, monitoring temperature-sensitive electrical parameters (TSEP) proves to be interesting, and among TSEP, the gate resistance (R_{gin}) is particularly relevant [7]. Estimating the junction temperature from R_{gin} involves a calibration phase to determine the function linking the read TSEP and temperature, followed by the application of direct current (DC) to the system's gate and measuring the voltage between the gate and the emitter to estimate the temperature using the calibration function. The equivalent circuit is generally modeled by an RC circuit, as illustrated in Figure 3. A related method, called "Tjbalancing,"



$$R_{gin}(T_j) = (\delta R_g \cdot T_j + 1) \cdot R_{g0}$$

$$V_{ge}(t) = R_{gin} \cdot I_g + \frac{t}{C_{ies}} \cdot I_g$$

Fig. 3: Equivalent circuit with TSEP R_{gin} (left) and signal shape during I_g current injection (right) [7].

stands out for its use in systems with multiple chips in parallel [8]. This technique provides real-time estimation of the junction temperature for each chip using the TSEP R_{gin} . It then thermally balances the chips by individually modifying the commands of the components, thus mitigating temperature disparities between them.

Monitoring temperature variations resulting from potential failures can enable precise localization of issues and contribute to the proactive maintenance of power electronic systems.

3 Methodology

This section presents the general methodology for determining the EI of a PE product, taking into account replacement due to system faults, the use of diagnostic technology for more or less precise fault detection, and modularity. Figure 4 illustrates the methodology for creating the staircase curve figure 1. For manufacturing, an inventory of material flows and processes is conducted. For usage, the EI concern the energy lost during operation, and a typical operating cycle (e.g. WLTP for automotive application) with a loss model is used [9]. The EI related to manufacturing and usage are not further detailed in the document. The replacement modeling includes fault generation and diagnostic processes that allow for defining replacement scenarios.

The replacement modeling implies the concept of the Replacement Unit (RU), representing the smallest replaceable component in the system. It is crucial to clearly define this RU, as this definition guides the methodology. For example, in the case of a three-phase inverter built with discrete components such as TO247, the RU could be the discrete component itself. However, the same inverter built using an integrated power module would have the entire module as the RU.

3.1 Diagnostic : Replacement matrix

The objective of this section is to create replacement scenarios, i.e., for each fault, what replacement choice the diagnostic allows. To achieve this, we generate a matrix called the "Replacement Matrix (RM)." This matrix is an input to the algorithm shown in Figure 4.

To develop this matrix, it is necessary to model the observation of the diagnostic for each type of fault. Depending on the observation, the diagnostic can deduce the location of the failure, and the deduced part is then replaced, thus forming a replacement scenario. It is essential to understand the consequences of faults, as well as the perspective of the diagnostic. A fault tree can be constructed to link the fault, the effects, the observations of the effects, and the replacement scenario. If the same observation is made for failures of several/all RU, then the several/all RU need replacement. If an observed effect is linked to a specific RU or group of RU, then only the RU or the group is replaced. The replacement matrix $[RM]$ specific to a diagnostic technique (l) can then be constructed as shown in Figure 5. RU_i represents replacement unit i ranging from 1

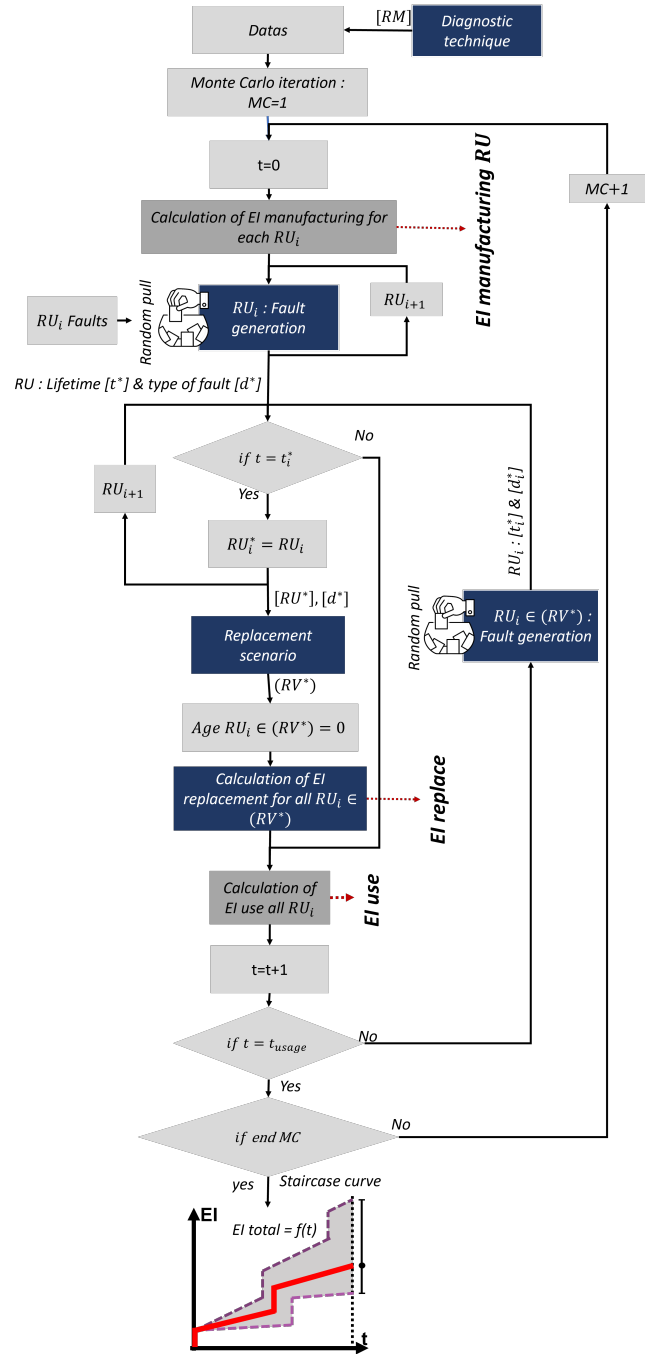


Fig. 4: Product life modelling with replacement and diagnostic.

to m , and $d_{k,i}$ represents fault k of replacement unit i , with a total number of faults of $n * m$ where n is the number of listed faults. The columns of the matrix are denoted by i and the rows by $j = k, i$. The replacement matrix is filled with 0 and 1, where 0 means no change is made, and 1 indicates a replacement. For example, in the matrix 5, if fault d_{11} of type 1 occurs on RU_1 , only RU_1 is replaced, indicating high diagnostic accuracy for this specific fault. However, if fault d_{21} of type 2 occurs on RU_1 ,

$$[RM]_{(l)} = \begin{matrix} & \overbrace{\begin{matrix} RU_1 & RU_2 & \dots & RU_m \end{matrix}}^i \\ \begin{matrix} 1 & 0 & \dots & 0 \\ 1 & 1 & \ddots & 0 \\ \vdots & \ddots & \ddots & \vdots \\ 1 & 1 & \ddots & 1 \\ 0 & 1 & \ddots & 0 \\ \vdots & \ddots & \ddots & \vdots \\ \dots & \dots & \dots & \dots \end{matrix} & \left. \begin{matrix} d_{1,1} \\ d_{2,1} \\ \vdots \\ d_{n,1} \\ d_{1,2} \\ \vdots \\ d_{n,m} \end{matrix} \right\} k, i = j \end{matrix}$$

Fig. 5: Replacement matrix generated from the fault tree, specific to a diagnostic type (l).

the diagnostic is less precise, and both $RU1$ and $RU2$ are replaced.

Each diagnostic technique has its own replacement matrix; they do not all have the same precision, some may better target the fault and result in fewer replacements for repair.

3.2 Fault Generation

First, an exhaustive list of all potential fault types for each RU needs to be established, along with determining the probability of the fault occurring over time. For example, a fault for a power chip could be a short circuit. The vector d of size $n * m$ with n as the total number of faults and m as the number of RU can be created as follows:

$$(d) = \begin{pmatrix} d_{k,i} \\ \vdots \\ d_{n,m} \end{pmatrix} \quad (1)$$

With k as the fault number and i as the RU number. Mathematically, faults can be modeled based on statistical laws. The Weibull function is the one selected (with two parameters σ and β), equation 2, as it allows for reproducing the "bathtub curve". This curve characterizes the different failure phases during the product's lifetime (LT) of a PE product [10], encompassing the "infant mortality" phase $\beta < 1$ (related to insufficiently controlled design or manufacturing issues), the "useful life" period $\beta = 1$ (where failures occur independently of the component's age), and the "aging" stage $\beta > 1$ (resulting from wearout). The distribution function of each fault k is written in the form:

$$f_k(t) = 1 - e^{-\left(\frac{t}{\sigma}\right)^\beta} \quad (2)$$

The algorithm for determining the fault type is presented in Figure 7, it consists of two key steps: fault generation and fault type selection.

Firstly, it is necessary to find the overall distribution function of the RU. It is necessary to associate faults within a RU, several types of associations exist [11]. Here, the series association is selected, meaning all subsystems must function for the overall system to be operational. In other words, there should be no faults, represented by the distribution function of an RU equation 3.

$$F_i(t) = 1 - \prod_{k=1}^n (1 - f_{k,i}(t)) \quad (3)$$

With $f_{k,i}$ being the distribution function of fault k of RU i and n the total number of faults for the RU. A random number compared to the RU's distribution function determines the fault time (t_i^*). A second random number is used to select the fault type ($d_{k,i}^* = d_j^*$), based on the probabilities associated with each type at the time of the fault. This algorithm allows for each RU, both to determine the time at which a fault occurs (t_i^*) and also, what type of fault occurs (d_i^*). This enables the generation of two vectors t^* and d^* of size m representing respectively the occurrence times and the fault types for each RU.

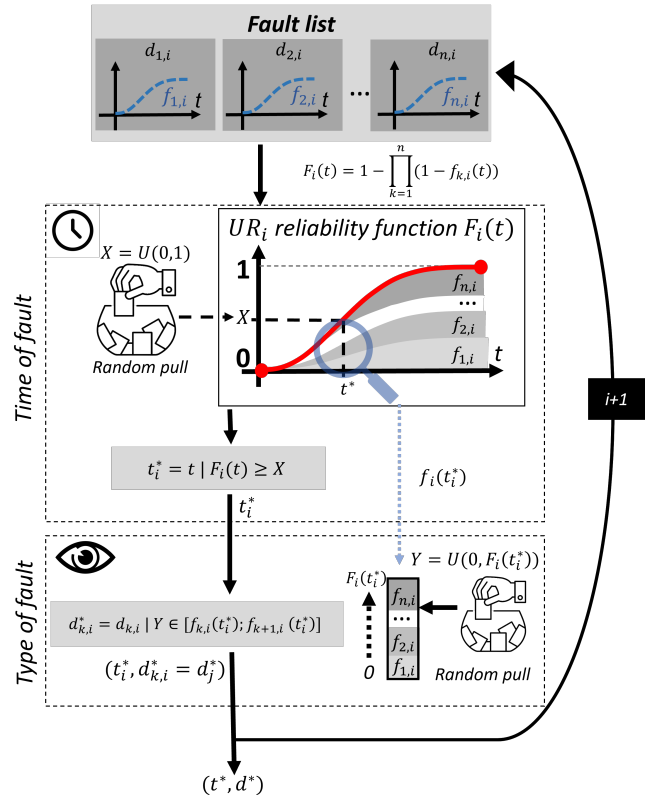


Fig. 6: Algorithm for generating a replacement unit fault.

3.3 Replace

The previous sections describe, on one hand, the creation of the replacement matrix based on faults and diagnostics for the input data, and on the other hand, the fault generation.

To calculate the EI related to replacement, it remains to link the two. For this purpose, depending on the fault type at a given time t , we will generate a replacement vector formed by a logical "OR" operation of all faults generated from the replacement matrix at time t^* , to avoid counting the replacement of a RU twice. This is expressed mathematically as follows:

$$RM^*(j, :) = \begin{cases} RM(j, :) & \text{if } d^*(i^*) = d(j) \\ 0 & \text{otherwise} \end{cases} \quad (4)$$

Where i^* represents the RU_i in fault, d^* the faults at t^* and d the vector of all type of faults.

$$(RV^*) = \bigvee_{j=1}^{m \times n} RM^*(j, :) \quad (5)$$

Where RV^* represents the replacement vector when a fault arrives at t^* , \bigvee the logical OR operator, and $RM^*(j, :)$ is the j -th line of RM^* .

Let's take an example: at time $t^* = t$, $RU1$ undergoes d_{21} , and $RU2$ undergoes fault d_{12} . The corresponding lines of the replacement matrix are as follows:

$$[RM^*] = \begin{array}{cccc|c} & RU_1 & RU_2 & \dots & RU_m & \\ \hline & 0 & 0 & \dots & 0 & d_{1,1} \\ & \mathbf{1} & \mathbf{1} & \ddots & \mathbf{0} & d_{2,1} \\ & \vdots & \ddots & \ddots & \vdots & \\ & 0 & 0 & \ddots & 0 & d_{n,1} \\ & \mathbf{0} & \mathbf{1} & \ddots & \mathbf{0} & d_{1,2} \\ & \vdots & \ddots & \ddots & \vdots & \\ & 0 & 0 & \dots & 0 & d_{n,m} \end{array}$$

Fig. 7: Example with $RU1$ undergoing d_{21} and $RU2$ undergoing d_{12} at time t .

The diagnosis indicates the need to replace $RU1$ and $RU2$. Using a logical OR, we obtain the following replacement vector:

$$(RV^*) = (1 \ 1 \ \dots \ 0) \quad (6)$$

Then, simply perform the matrix calculation of the replacement vector with the matrix of EI for the manufacturing of each component:

$$EI_{\text{replace}}(t) = (RV^*) \cdot (EI_{mf}) \quad (7)$$

$$(EI_{mf}) = \begin{pmatrix} EI_{mf} \text{ RU1} \\ EI_{mf} \text{ RU2} \\ \dots \\ EI_{mf} \text{ RU}_m \end{pmatrix} \quad (8)$$

With EI_{mf} representing the environmental impacts during manufacturing.

In conclusion, the developed methodology provides an approach to evaluate the EI related to the replacement of a PE system subdivided into RU. Through fault generation, determination of fault type, modeling of replacement scenarios via a diagnostic-dependent replacement matrix, and finally the calculation of EI associated with these replacements.

4 Case studies

To illustrate the method and quantify the environmental benefits of implementing modularity and diagnosability, a case study is developed here.

4.1 Systems studied: modularity and diagnostics

The analysis compare two topologies comprising an IGBT conversion cell and its gate control board (driver). One is the "integrated" topology, illustrated in Figure 8, and the other is the "discrete" topology, represented in Figure 9 (a and b), which represents our modular cases.

The **integrated** topology is characterized by 2 RU, an IGBT power module consisting of six IGBT chips and six diodes, along with a control board. The power module is the FS820R08A6P2B (750V, 820A) with its driver, as presented in reference [9]. For the discrete topology, 2 proposals are studied:

Discrete (1): The simplest simplification involves virtually splitting the integrated topology into 6 parts, where the total EI for manufacturing remains identical to those of the integrated one. However, there are now 12 replacement units (RU), including 6 components and 6 drivers, sharing these impacts.

Discrete (2): Represents a more realistic modeling of a modular system compatible with current rating of discrete component. It consists of 48 RU, including 24 discrete components and 24 drivers. The chips are paralleled four by four, each with its driver. The IGBTs are packaged in TO247, similar to the inverter of the Tesla Model S. The IGBT chip and the diode are in the same package, with a rating of 205A and a nominal voltage of 750V. The EI for the manufacturing of the IGBTs are deduced from the specific LCA of the TO247, which is not developed in the article. As for the drivers, given the lack

of examples of discrete drivers, an assumption is made regarding their form, representing them in the form of cells arranged on the same printed circuit board, maintained at a sufficient distance to allow access without damaging neighboring cells in case of repair of the faulty component. This assumption is inspired by the proposal of standard conversion cells presented in reference [12], allowing individual repairs of the cells. The total EI for manufacturing of the drivers are considered equivalent to those of the integrated driver. Each driver RU evenly shares the total EI for manufacturing.

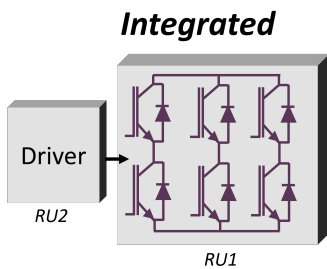


Fig. 8: Integrated topology.

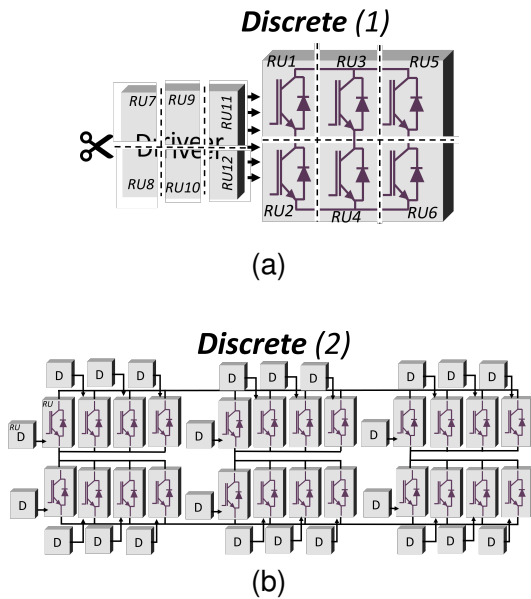


Fig. 9: Discrete topologies (1) and (2) of the case study.

4.2 Default type and probability

Based on a literature review [13], [14], a list of failures has been established for IGBT chips and drivers, with information regarding the stages of infancy, useful life, and end of life, all presented in Table 1.

Current literature presents limited availability of data regarding the parameters σ and β of the Weibull functions used to model the faults. The three functions for infancy (Early-E), useful life (Random - R), and aging (Wearout - W) are modeled separately, and the values of the three functions are shown in Figure 10.

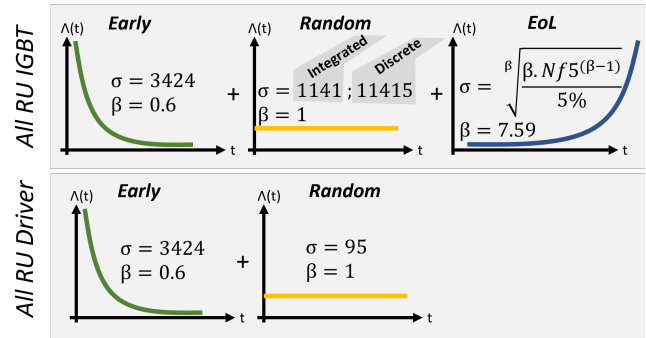


Fig. 10: Selected default probability functions.

The parameters for infancy-related faults are obtained from a reference at Semikron [15]. The values correspond to the entire PE system, with $\beta = 0.6$ and $\sigma = 3424$ years. In our case, these represent the values of the overall reliability function of the (IGBT+driver) for infancy-related faults.

The faults related to the useful life period all have $\beta = 1$. For the useful life faults of the integrated power module, the parameters used are derived from references [16]–[18]. σ is determined from the FIT (1 FIT corresponds to 1 failure per 10^9 hours). The total FIT of the power module (=100, so $\sigma = 1141$ years) appears to be 10 times higher than that of a discrete component, which is $\sigma = 11415$ years. This is logical, as the discrete IGBT RU consists of only one chip, hence less chance of experiencing failures.

For driver faults, the total number of FITs was set at 1200 [19], which corresponds to 95 years. The FIT of the integrated driver or the discrete driver is considered to be the same.

The parameters for end-of-life faults only concern the IGBT RU, with the modeling of system degradation, both for the IGBT chip and the diode. The values are determined from the chip lifetimes [20]. Firstly, input data are defined, including product usage (operating cycle) and component physics (electrical parameters, thermal parameters, and its lifetime model). Then, the input data are implemented into a loss model. The losses are used to calculate the junction temperature rise using a

thermal model. A counting algorithm determines the number of temperature cycles undergone by the component, which are then compared to the lifetime model. This provides the maximum cycle number until failure denoted as Nf_5 , with the 5 indicating the failure rate to create the empirical model, i.e., 5% of the failed sample.

Using the functions for each RU, equation 3 allows retrieving the values of individual faults. Table 1 presents the different values obtained for each fault depending on the topology.

4.3 Diagnostic technique and replacement scenario

For the case study, both diagnostic techniques presented are utilized, namely the basic **desat** technique and **Tjbalancing** (which also implements desat technique).

Based on the selected techniques and as explained in the method, it is essential to model the diagnostic observation for each fault, which is not detailed in the article. Table 1 presents the replacement scenarios according to the type of fault and the diagnostic technique used. They are equivalent to the replacement matrix in 5.

4.4 Results

Figure 11 illustrates the evolution of the Mineral and Metal Resource Depletion (MRD) environmental impact over time for integrated and discrete topologies, taking into account fault generation and diagnosis (according to the probabilistic method presented earlier). MRD is presented because it is the impact most affected by manufacturing and replacement [9]. Additionally, the curves represent the median values of the 1000 Monte-Carlo simulations.

We can observe that diagnosis and modularity have little impact on the curves between integrated and discrete, as the entire system is replaced at 30 years. This is due to the type of fault, primarily related to wearout. Thus, the curves corresponding to integrated (desat and Tjbalancing) and discrete (1) (desat and Tjbalancing) have the same EI at 30 years, as both systems are entirely replaced once. The discrete solution (2) is the most polluting (9% higher than integrated), but this is solely explained by the manufacturing EI, which is more costly (26%).

Adding diagnostic functions is not always a solution to reduce EI. For this to be the case, the entire system should not be systematically replaced. Even if

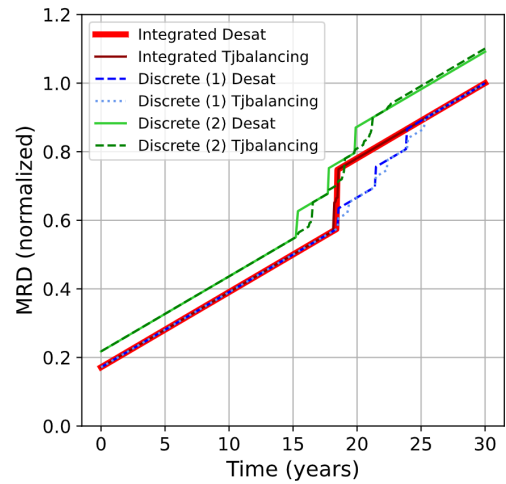


Fig. 11: Impact of diagnostics and modularity on MRD.

diagnosis allows for locating the fault and replacing only the faulty component, it brings no benefit in terms of EI if other components are also likely to fail shortly after.

This is why diagnosis is particularly relevant for faults related to the youth or useful life of the system, while faults related to wearout do not present significant interest, as the failure of one chip will likely be followed by failures of other chips in the system.

The data used for modeling faults were probably not representative of the actual probability of occurrence of faults, mainly due to a lack of in-depth studies in this area. Therefore, a definitive conclusion on the real interest of diagnosis and modularity cannot be formulated at this stage.

Having no precise vision of whether a fault will occur or not, we will now focus on the impacts of diagnosis and modularity depending on the type of fault.

According to the faults studied and the RU, based on Table 1, there are 4 levels of Fault Location Identification (FLI):

- Without FLI (e): The fault cannot be localized, resulting in the replacement of the entire system.
- Low FLI (d): Fault is localized at the level of one power arm with the associated drivers for that arm.
- Moderate FLI (c): Fault is localized at the level of one power switch with its driver.
- Strong FLI precisely localized at the level of

Tab. 1: Type and probability of fault for each RU in the case study, with replacement scenario.

RUi	Fault	Life period	Weibull				Replacement scenario	
			σ (years)			β	Desat	Tjbalancing
			Integrated	Discret (1)	Discret (2)			
IGBT	DC bus disconnection	Early	50 060	991 750	9 996 220	0.6	d	c
	Load disconnection		50 060	991 750	9 996 220	0.6	d	c
	Bad thermal interface		50 060	991 750	9 996 220	0.6	d	b
	Die SC IGBT	Random	4 564	45 660	45 660	1	d	d
	Die OC IGBT		4 564	45 660	45 660	1	d	b
	Die SC diode		4 564	45 660	45 660	1	d	d
	Die OC diode		4 564	45 660	45 660	1	d	d
	IGBT degradation of the wire-bonds/ Degradation of the die-attach	End of life	22.8	28.9	28.9	7.59	d	b
	Diode degradation of the wire-bonds/ Degradation of the die-attach		20.4	25.8	25.8	7.59	d	d
Driver	Control board disconnection	Early	50 060	991 750	9 996 220	0.6	e	c
	Grid disconnection		50 060	991 750	9 996 220	0.6	d	a
	Fault in high state (commands IGBT to close)	Random	190	570	2280	1	d	a
	Fault in Low state(commands IGBT to open)		190	570	2280	1	e	c

Legend : Replace specific Driver (Strong FLI - a), Replace specific IGBT (Strong FLI - b), Replace specific IGBT and its Driver (Moderate FLI - c), Replace all IGBTs and Drivers leg (Low FLI - d), Replace all (Without FLI - e)

the power component alone or at the level of the driver alone.

The impact of these FLI levels on replacement is directly related to modularity. For example, in the case of moderate-level FLI, which corresponds to the following information: when a fault occurs, it may involve both the power component and its driver. In this scenario, for discrete topology (1), the specific IGBT and its driver are replaced, while for integrated topology, the entire system is changed because the RU do not allow for separation, even if information about the fault location is obtained. Furthermore, the Tjbalancing diagnostic technique allows for precise RU selection for certain faults, unlike the desat technique, which stops at the power arm level, thus offering less fine resolution. Knowing this, the cost of replacement for different FLI levels and different topologies is determined, as shown in Figure 12. The EI at replacement of the integrated case without FLI is taken as a reference. Comparing the EI of the fault without FLI simply shows the difference in the system's manufacturing cost, as everything is replaced here. With the desat technique, when a fault with low FLI occurs, modularity reduces the EI at replacement compared to the integrated case by 67% (discrete(1)), 36% (discrete(2)). With the implementation of the Tjbalancing technique, the positive impact of modularity further increases. For faults with moderate FLI, there is a reduction of 83% (discrete(1)), 91% (discrete(2)). For faults with strong FLI, a reduction of 90% (discrete(1)), 92% (discrete(2)). In contrast, the integrated model achieves only a 37% reduction

at replacement for faults with strong FLI. So, having an accurate FLI benefits more to the most modular system, namely the discrete (2). Further studies

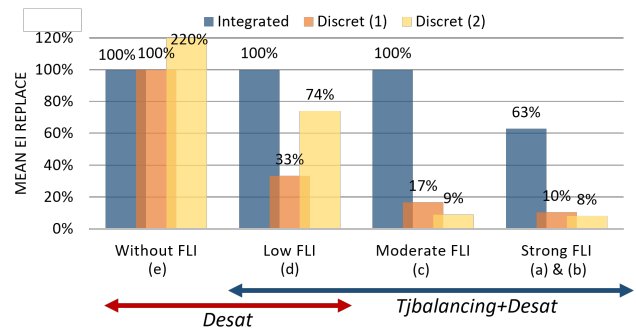


Fig. 12: EI at replacement between different modularities for different FLI, standardized EI compared to replacement of integrated without FLI.

are needed to determine the actual occurrence of faults and thus assess their diagnostic level, in order to conclude on the real utility of diagnostics and modularity. If, in reality, the most common faults are related to wearout, then diagnostics do not present a significant advantage. However, if the most frequent faults are those that can be located accurately and occur when the other parts of the system have high value (i.e. reliability), then it is worth to replace the single failed RU and modularity and diagnosability become relevant characteristics. To illustrate this point, Figure 13 highlights the impact of diagnostics and modularity on MRD over time. Three faults are simulated, occurring at 10, 15, and 25 years for each topology. Each fault corresponds to a certain FLI level; for example, the

strong FLI level is represented by the failure of the thermal interface, leading to the replacement of the specific IGBT RU.

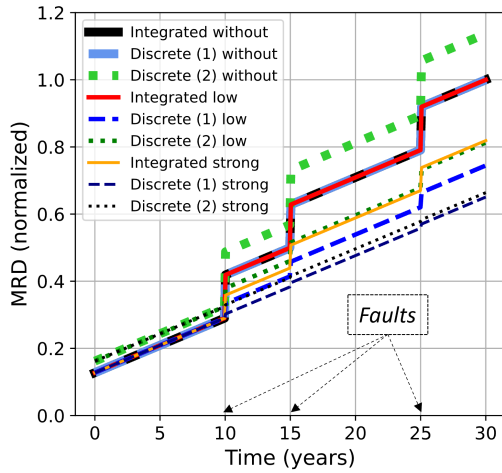


Fig. 13: Impact of diagnostics and modularity on MRD, in the proposed 3-defect scenario.

As previously mentioned, without FLI, the difference is related to the manufacturing cost; modularity does not influence, with integrated and discrete (1) being at the same level, while discrete (2), with a higher manufacturing cost, increases MRD by 13% at 30 years. For a low diagnostic level, the total MRD reduction compared to the integrated case without diagnostics at 30 years is 25% and 18% respectively for discrete solutions (1) and (2). With a high diagnostic level, the total MRD reduction is 34% and 33%, but also 18% for the integrated solution with high diagnostics. Thus, two aspects emerge: the impact of diagnostics and that of modularity.

Figure 14 shows the same results at 30 years for all EI with environmental gain for different topologies with different FLI levels. The results are normalized relative to the integrated scenario without FLI information. When faults lead to strong FLI, all discrete topologies show a reduction in EI. However, for most EI, this reduction is low ($< 5\%$), mainly due to the significant contribution of the usage phase compared to manufacturing [9]. Also, discrete topology (2) leads to a significant increase in EI in the absence of FLI during a fault, with an increase of 47% for OD, 14% for HT, etc.

5 Conclusion

We have discussed some aspects of modularity and diagnosability in PE. Our approach involved

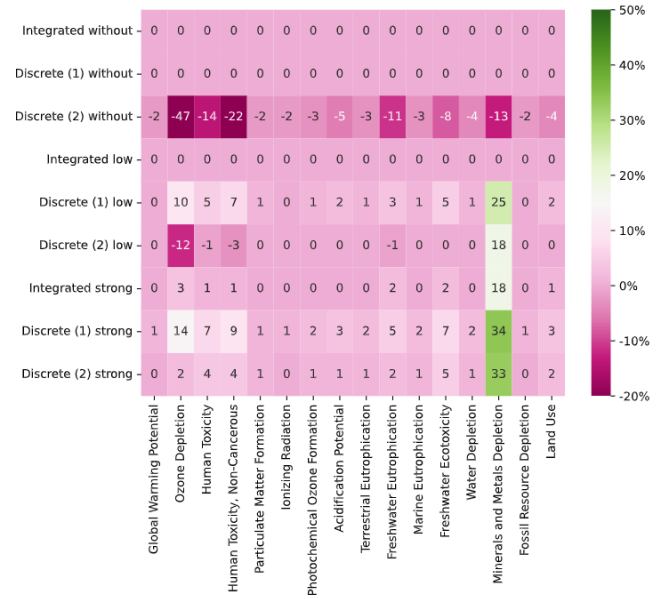


Fig. 14: Percentage gain (%) for each EI at 30 years of the different topologies with the different FLI levels compared with the integrated case with no FLI information.

a methodology for modeling EI integrating modularity and diagnosability. This method provides a modular view through RU, the smallest entities that can be replaced. It requires a thorough study of defects specific to each type of RU. The methodology implements a fault generation procedure and confronts them with diagnostic techniques to propose a replacement scenario for quantifying the EI.

An inverter composed only of power components and drivers served as a case study to implement this methodology, with one non-modular (integrated) topology and two modular topologies (discrete). The analysis of the results highlighted the influence of topology choice, as well as the presence or absence of diagnostics, on environmental indicators such as Mineral and Metal Resource Depletion (MRD).

Modularity and diagnostics have been found to be factors enabling EI reduction by targeting specific faulty components, although this reduction is not always guaranteed under all conditions. It is essential to note that the actual effectiveness of diagnostics and modularity depends on the frequency and type of faults observed, the easier to localize the faults, the more modularity will enable EI reduction. Also, we observed that, for wear-out faults, diagnostics may not bring significant improvement compared to an approach without diagnostics, as in all cases,

the entire system is replaced. In an industrial context, this is relevant because converters are sized not to have wearout failures over the product's lifetime thanks to adequate cooling sizing for product usage.

The current case-study concentrates on the power semi-conductor devices and gate drivers only, which represent around 1/3rd of the MRD impact of a complete inverter [9]. Inverter-level modularity, to provide dismantability from other key components such as the casing and capacitors, may present additional advantages than can be addressed with the proposed methodology. Current literature presents limited availability of data regarding the σ and β parameters of Weibull functions used to model faults. Therefore, the different data used come from various sources and may not always precisely match the studied fault not the target application. Future research should thus focus on more comprehensive and application-specific data collection to assess the actual occurrence of faults and perform the life-cycle assessment of modularity and diagnosticability.

References

- [1] M. Sonogo, M. E. S. Echeveste, and H. Galvan Debarba, "The role of modularity in sustainable design: A systematic review," *Journal of Cleaner Production*, vol. 176, pp. 196–209, Mar. 2018. DOI: 10.1016/j.jclepro.2017.12.106.
- [2] Y. Yang, L. Dorn-Gomba, R. Rodriguez, C. Mak, and A. Emadi, "Automotive Power Module Packaging: Current Status and Future Trends," *IEEE Access*, vol. 8, pp. 160 126–160 144, 2020. DOI: 10.1109/ACCESS.2020.3019775.
- [3] C. Buttay, "Le Packaging en électronique de puissance," fr, 2015.
- [4] T. T. Romano, T. Alix, Y. Lembeye, N. Perry, and J.-C. Crebier, "Towards circular power electronics in the perspective of modularity," *Procedia CIRP*, CIRP, vol. 116, pp. 588–593, Jan. 2023. DOI: 10.1016/j.procir.2023.02.099.
- [5] S. Lefebvre and B. Multon, *MOSFET et IGBT : Circuits de commande*, fr, 2003.
- [6] L. Foube, "Power Devices Health Condition Monitoring: A Review of Recent Papers," en, *PHM Society European Conference*, vol. 6, no. 1, pp. 15–15, Jun. 2021, Number: 1. DOI: 10.36001/phme.2021.v6i1.2808.
- [7] J. Brandelero, J. Ewanchuk, and S. Mollov, "Online Virtual Junction Temperature Measurement via DC Gate Current Injection," in *CIPS 2018*, Mar. 2018, pp. 1–7.
- [8] J. Brandelero, J. Ewanchuk, N. Degrenne, and S. Mollov, "Lifetime extension through Tj equalisation by use of intelligent gate driver with multi-chip power module," *Microelectronics Reliability*, vol. 88-90, pp. 428–432, Sep. 2018. DOI: 10.1016/j.microrel.2018.07.034.
- [9] B. Baudais, H. Ben Ahmed, G. Jodin, N. Degrenne, and S. Lefebvre, "Life Cycle Assessment of a 150 kW Electronic Power Inverter," en, *Energies*, vol. 16, no. 5, p. 2192, Jan. 2023, Number: 5 Publisher: Multidisciplinary Digital Publishing Institute. DOI: 10.3390/en16052192.
- [10] P. Blanquart and J.-c. Ronclin, *Fiabilité*, fr, 1989.
- [11] T. T. L. Pham, "Contribution à l'étude de nouveaux convertisseurs sécurisés à tolérance de panne pour systèmes critiques à haute performance. Application à un PFC Double-Boost 5 Niveaux," fr, Ph.D. dissertation, INPT, Nov. 2011. DOI: 10/document.
- [12] M. Rio, K. Khannoussi, J.-C. Crebier, and Y. Lembeye, "Addressing Circularity to Product Designers: Application to a Multi-Cell Power Electronics Converter," in *CIRP 2020*, ELSEVIER, May 2020. DOI: 10.1016/j.procir.2020.02.158.
- [13] F. Richardeau and A. Gaillard, *Modes de défauts principaux et principes de sécurisation de l'onduleur de tension*, fr, 2017.
- [14] A. Abuelnaga, M. Narimani, and A. Bahman, "A Review on IGBT Module Failure modes and Lifetime Testing," *IEEE Access*, vol. PP, pp. 1–1, Jan. 2021. DOI: 10.1109/ACCESS.2021.3049738.
- [15] U. Scheuermann, *How to Define the Adequate Reliability Requirement for a Power Electronic System?* 2012.
- [16] Infineon, *FIT-Rate Report FS820R08A6P2x*, 2022.
- [17] I. Corporation, *RELIABILITY REPORT 2016 Power Semiconductor Devices*, 2016.
- [18] Infineon, *FIT Failure Rate of AUJRG4066D1-E*, 2022.
- [19] J. Wylie, M. C. Merlin, and T. C. Green, "Analysis of the effects from constant random and wear-out failures of sub-modules within a modular multi-level converter with varying maintenance periods," in *EPE'17 ECCE Europe*, Sep. 2017, P.1–P.10. DOI: 10.23919/EPE17ECCEurope.2017.8099246.
- [20] N. Degrenne and S. Mollov, "Real-life vs. standard driving cycles and implications on EV power electronic reliability," in *IECON 2016*, Oct. 2016, pp. 2177–2182. DOI: 10.1109/IECON.2016.7793633.